

Original Research

## Implementation of a Dynamic Thermal and Illuminance Control System in Responsive Façades: Shading Study

Gabriel de Bem <sup>1,2,3</sup>, Marlon Mühlbauer <sup>3</sup>, Pablo La Roche <sup>1</sup>, André Matias <sup>4</sup>, Ricardo Almeida <sup>4</sup>, Eduardo Krüger <sup>2,\*</sup>

1. California State Polytechnic University – Pomona, California, United States of America; E-Mails: [gabriel.bem@ifsc.edu.br](mailto:gabriel.bem@ifsc.edu.br); [pmlaroche@cpp.edu](mailto:pmlaroche@cpp.edu)
2. Federal University of Technology – Paraná, Brazil; E-Mail: [ekruger@utfpr.edu.br](mailto:ekruger@utfpr.edu.br)
3. Federal Institute of Education, Science, and Technology – Santa Catarina, Brazil; E-Mail: [marlon.mulhbauer@ifsc.edu.br](mailto:marlon.mulhbauer@ifsc.edu.br)
4. Polytechnic Institute of Viseu – Viseu, Portugal; E-Mails: [andre Luis.matias21@gmail.com](mailto:andre Luis.matias21@gmail.com); [ralmeida@estgv.ipv.pt](mailto:ralmeida@estgv.ipv.pt)

\* **Correspondence:** Eduardo Krüger; E-Mail: [ekruger@utfpr.edu.br](mailto:ekruger@utfpr.edu.br)

**Academic Editor:** Francesco Leccese

**Special Issue:** [Energy – Urban Planning and Sustainable Development](#)

*Adv Environ Eng Res*

2022, volume 3, issue 3

doi:10.21926/aer.2203038

**Received:** May 30, 2022

**Accepted:** September 18, 2022

**Published:** September 29, 2022

### Abstract

This study evaluates three shading configurations designed and tested in a preliminary stage of responsive shading device development. The strategy is based on trigonometric relationships focused on solar angles at any given moment. The configurations are thus related to the ratio of the window area shaded by a responsive brise-soleil that provides 0%, 50%, or 100% shading of the indoor space, based on the daylight needs and the indoor thermal control realized. Shading simulations were performed for Pomona, California (latitude 34.04°) for different seasons of the year. Simplified thermal simulations were run in EnergyPlus to estimate the effectiveness of the method in a full-scale environment of three shading modes (static shading device, seasonal shading, and responsive brise soleil). Comparisons were made relative to a 'no shading' condition to improve indoor comfort



© 2022 by the author. This is an open access article distributed under the conditions of the [Creative Commons by Attribution License](#), which permits unrestricted use, distribution, and reproduction in any medium or format, provided the original work is correctly cited.

conditions. The results of the visual analysis demonstrated a higher shading efficiency for lower solar angles between the equinoxes and winter. In terms of comfort, the response brise soleil was found to be promising in locations with seasonal variations. The response was low in predominantly tropical climates. Therefore, the strategy can be used to better control indoor conditions. The extent of solar heat gain and the degree of work-task illuminance can be improved to improve comfort in naturally conditioned spaces. The extent of energy consumption can be reduced.

### Keywords

Responsive architecture; UDI; illuminance control; dynamic façade; shading; thermal performance analysis

## 1. Introduction

The function of a given building is subject to change throughout its life cycle due to changes in occupancy and users' needs. Passive strategies cannot cope with this dynamic demand [1]. Moreover, dealing with daily and seasonal weather variations (changes in radiation intensity and solar position, wind speed and direction, variations in humidity and outdoor temperature) with static and passive solutions can be a complex task [2].

According to Meagher, “[...] responsive components encompass all the parts of the building that are able to adapt and change in response to the environment or to accommodate the contingencies of daily life” [3]. One of the primary purposes of a responsive building is to maintain indoor environmental quality (IEQ). This process can be achieved by developing mechanical elements that can control openings (windows, doors, and vents) and shading devices (louvers, sunshades, and screens) [3]. Responsive, constructive elements can be associated with cross ventilation, direct sunlight, and daylight illuminance management. The functions of the elements will eventually impact the building's thermal performance and user comfort.

Matin and Eydgahi [4] simulated the luminous performance of an office room by comparing three different conditions: non-shaded, fixed louvers (horizontal and vertical) and responsive façade with horizontal and vertical louvers. The system was set to change the orientation every hour based on an algorithm. The aim was to find the optimal tilt angle to improve indoor illuminance. Results obtained from the responsive façade were significantly better than those obtained using other models. Shading can also control night ventilation and thermal mass to improve indoor temperature under different climate conditions. These properties were studied by La Roche and Murray [5] and Kuczyński et al. [6] for warm and temperate climates, respectively. In both studies, the blinds were considered to be completely open or fully closed. The dynamic shading system reported herein is significantly improved and can help advance this field of research.

Daylight gains in buildings should ensure the well-being of the occupants. Phillips [7] stated that work environments devoid of natural light could lead to health problems, and under these conditions, the productivity of the occupants decreases. Exposure to daylight affects the whole body, including the skin and eyes. It also affects psychological responses and hormone production

and helps to reduce stress and discomfort [8]. An indoor environment that relies on manageable natural light tends to be healthier and contributes to user comfort and building performance. Furthermore, the demand for artificial lighting and space conditioning decreases. According to the International Energy Agency (IEA) reports, electricity corresponds to 33% of the total energy demand in the building sector. Recent advances made in terms of increased energy efficiency in buildings have helped the growth of the building sector. Further development of the field required the development of measures to achieve Net Zero Emissions (NZE) by 2050, a normative scenario proposed by IEA [9].

A responsive façade that can adapt its openings to improve IEQ under conditions of dynamic changes in atmospheric conditions presents itself as a promising solution to building sustainability [10]. Better use of natural light can reduce the electricity demand in the operational stage of the building. Controlling the extent of utilization of solar heat can improve indoor temperature and reduce the energy demand related to air conditioning. Reinhart reinforces the relevance and complexity of the subject matter: *“A daylight space is primarily lit with natural light and combines high occupant satisfaction with the visual and thermal environment with low overall energy usage for lighting, heating, and cooling”* [11].

The aim of the present study was to design and control responsive shading devices to ensure the optimal thermal and luminous performance of a test environment. The following sections of this paper describe the research flow (addressing the development of the mathematical equations that guide the control system), the 3D simulation of possible daylight scenarios, and a simulation-based thermal performance evaluation of the responsive shading system. Methods were used to study a full-scale test environment under three different climatic conditions. The novelty of the research lies in the development of a low-cost responsive shading system. The feasibility of using the developed system should be studied, among others, for the further development and implementation of the proposed method.

## 2. Materials and Methods

We explored three shading patterns for a responsive shading-slats system: 0%, 50%, and 100% shading of the glazed area. The three conditions are based on the position of the Sun, and the solar path (specifically, the solar angle) is tracked. The daylight performance was analyzed, and the research flow consisted of four steps: 1) determining the guiding shading equations, 2) setting acceptable thermal control parameters, 3) applying daylight availability and metrics to the guiding equations, and 4) performing 3D modeling simulations. In addition, thermal simulations were run for a full-scale test environment to test the performance of the responsive shading system in three different climate regions of Brazil. The goal of the research is to find the optimal shading solutions for buildings in Brazil. Thermal simulations were conducted with EnergyPlus and the different conditions tested have been presented: 1) no shading device, 2) static shading device 3) seasonal shading device, and 4) responsive shading device (triggered by a reference setpoint temperature).

## 3. Daylight Performance Analysis

The effect of daylight was analyzed using a shading device (brise-soleil) that was designed at the test-cell facility at the Lyle Center, a Center for Regenerative Studies at California State Polytechnic University. The center is located at 34.05 °N and 117.82 °W in Pomona, California. The

test cell dimensions are 1.35 m × 1.35 m × 1.35 m, with a south-oriented window measuring 0.61 m × 0.61 m. The approximate window-to-wall ratio (WWR) is 40%. The walls are made of drywall studs with glass wool insulation, oriented standard board (OSB), thermal insulation boards made of polyisocyanurate (reinforced with aluminum foil (polyiso + aluminum)), and plywood (used to build the exterior). The wall thickness is 18 cm, and the U-value is 0.308 W/m<sup>2</sup>K. The floor is made of an OSB board inside, studs with glass wool insulation, and polyiso + aluminum insulation boards characterized by a U-value of 0.299 W/m<sup>2</sup>K. The roof consists of drywall, polyiso + aluminum insulation board, air gap, OSB, and waterproof liners covered with a metal sheet (U-value: 0.306 W/m<sup>2</sup>·K). Figure 1 presents the floor plan and cross-section of the test cell used for daylight analysis.

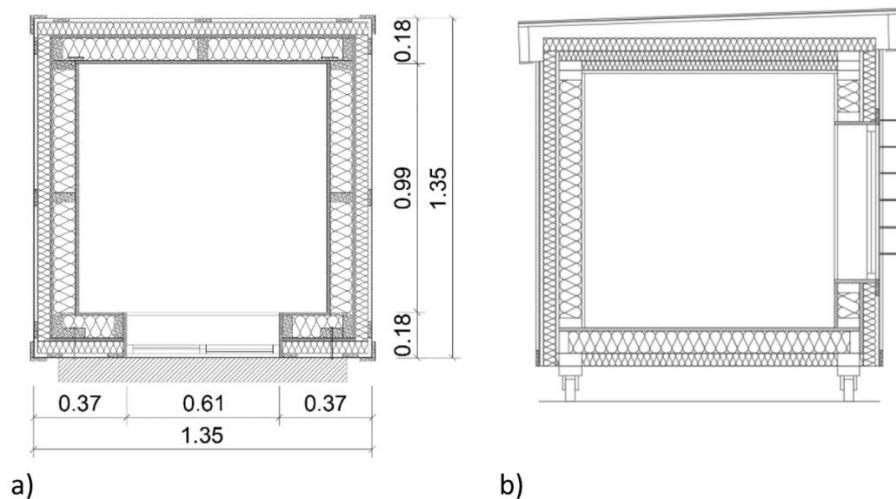


**Figure 1** floor plan (a) and cross-sectional view (b).

The shading simulations were performed in Sketch-Up<sup>1</sup>. Obstacles such as nearby trees and surrounding buildings were neglected.

### 3.1 Guiding Equations for the Control System

It is assumed that the shading device is tilted at different slats rotation angles ( $\Theta$ ) to allow or prevent the entry of direct sunlight (to provide sufficient illuminance under conditions of controlled solar heat gain) into the buildings. The calculations are based on trigonometric equations and the position of the sun. The following demonstration considers the solar path reaching the south façade with a solar azimuth of 180° (north hemisphere) at noon. Solar altitude ( $\alpha$ ) corresponds to the angle between the horizontal projection of the sun's position in the sky dome. The line formed by  $BA$  and  $CD$  corresponds to the louver slats in a horizontal projection. When the slats are rotated, the coordinates are  $BA'$  and  $CD'$ . The shading pattern and the respective equations have been presented.

<sup>1</sup>. SketchUp is a 3D design software structured on free learning resources and an intuitive design process developed by Trimble, an industrial technology company headquartered in California, U.S. The design software is available for use on the web, desktop, or iPad [12].

### 3.1.1 0% Shading

Under conditions of 0% shade, the entire window area receives direct sunlight. The louver slats rotation ( $\Theta$ ) should coincide with the solar altitude ( $\alpha$ ). The slat's thickness is the sole factor that determines shading under these conditions. Figure 2 shows a hypothetical example when  $\alpha = 36.12^\circ$ .

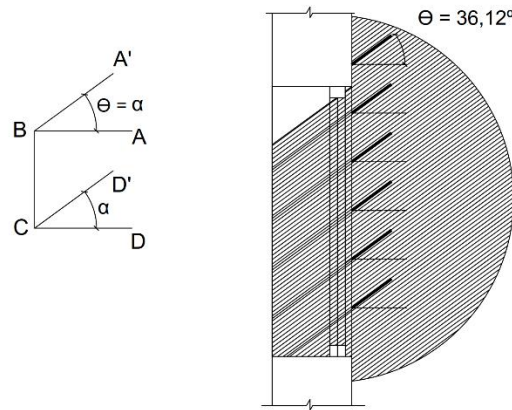


**Figure 2** 0% shading simulation for  $\alpha = 36.12^\circ$ .

This result is obtained as follows (equation 1):

$$\Theta = \alpha, \tag{1}$$

where  $\Theta$  is the angle of tilt of the louver slat and  $\alpha$  is the solar altitude angle.

This slat's position is controlled to increase the temperature and luminance levels. Counterclockwise rotation improves the indoor temperature under conditions of heat gain. This is especially true for the winter season. Under these conditions, the shading system behaves differently from other ordinary shading systems.

### 3.1.2 50% Shading

The hypothetical model considers that the depth of the louver slat ( $BA$ ) and the distance between the slats ( $BC$ ) are of the same dimensions ( $BA = BC = CD$ ) to achieve 50% shading in an indoor environment.  $E$  corresponds to the midpoint between  $B$  and  $C$  (Figure 3).

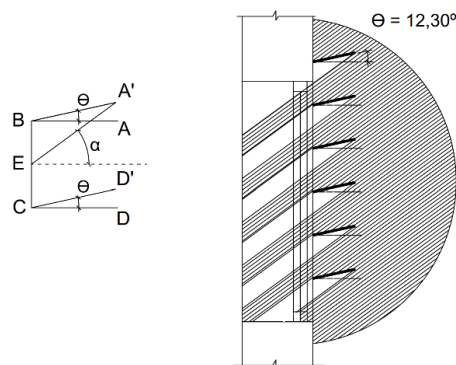


**Figure 3** Simulating the 50% shading conditions ( $\alpha = 36.12^\circ$ ).

The slat's tilt angle,  $\Theta$ , formed by  $BA'$ , should be such that the amount of sunlight reaching  $BC$  should be reduced to 50%. Under these conditions, the sunlight at  $BE$  should be blocked, allowing for the reduction of the thermal load at  $CE$  and the illuminance levels.

The triangle formed by  $EBA'$  is considered ( $\hat{B} = 90^\circ + \Theta$ ,  $\hat{E} = 90^\circ - \alpha$ ). As the sum of internal angles of a triangle is  $180^\circ$ ,  $\hat{A} = \alpha - \Theta$ .

Equation 2 is obtained based on the sine theorem and considering  $BA' = 2 \times BE$ :

$$\frac{BE}{\sin(\hat{A})} = \frac{BA'}{\sin(\hat{E})} \Rightarrow \frac{1}{\sin(\alpha - \theta)} = \frac{2}{\sin(90^\circ - \alpha)} \quad (2)$$

$\sin(90^\circ - \alpha)$  is replaced by  $\cos(\alpha)$ , and equation 3 is obtained as follows:

$$\theta = \alpha - \arcsin\left(\frac{\cos(\alpha)}{2}\right), \quad (3)$$

where  $\Theta$  is the angle of tilt of the louver slat and  $\alpha$  is the solar altitude angle.

This rotation angle allows 50% of the total window area to receive direct sunlight. This will likely occur when heat gain is still permitted (indoor conditions within the thermal comfort zone) and higher illuminance levels are required. For this case.  $\alpha = 36.12^\circ$  and  $\Theta = 12.30^\circ$  (slat's angle).

### 3.1.3 100% Shading

As in the previous case, the hypothetical model considers that the depth of the louver slat ( $BA$ ) and the distance between the slats ( $BC$ ) are of the same dimensions. The  $\Theta$ , in this case, rotates in a clockwise direction, and it is assumed that  $BA'$  and  $CD'$  block sunlight in  $BC$  (Figure 4).

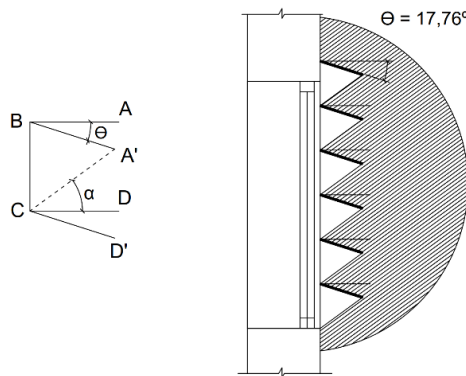


**Figure 4** Simulating the 100% shading condition ( $\alpha = 36.12^\circ$ ).

Assuming  $CBA'$  as an isosceles triangle,  $\hat{B} = 90^\circ - \Theta$  and  $\hat{C} = \hat{A}' = 90^\circ - \alpha$ . The sum of the internal angles of a triangle is  $180^\circ$  (equation 4), and  $\Theta$  is obtained from equations 4 and 5 as follows:

$$90^\circ - \theta + 2 \times (90^\circ - \alpha) = 180^\circ, \quad (4)$$

$$\theta = 90^\circ - 2\alpha, \quad (5)$$

where  $\Theta$  is the angle of tilt of the louver slat and  $\alpha$  is the solar altitude angle.

The rotation angle for the sun at an altitude of  $36.12^\circ$  corresponds to  $17.76^\circ$ , and this condition corresponds to full shade. This shading pattern prevents the entry of thermal loads and, at the same time, reduces the degree of indoor luminance. As the slats do not completely block the window (unless  $\Theta = 90^\circ$ ), even when there is 100% shading, the indoor environment is always subject to diffuse solar radiation, providing an outside view.

Whenever the value of  $\Theta$  is negative (counterclockwise rotation), the slats could remain in a horizontal position ( $\Theta = 0^\circ$ ). Under these conditions, the outside could be viewed under conditions of no louver interference (Figure S1 and Figure S2 - Additional material)). When the value of  $\Theta$  is positive, and the illuminance level remains above the upper threshold, additional angles (clockwise) can be set to reduce diffuse solar radiation.

As the guiding equations only consider the solar altitude angles for indoor shading, accurate results are obtained when the solar azimuth is close to  $180^\circ$ . This is because the trigonometric relation is based on a planar projection.

### 3.2 Thermal Control

For thermal control, the shading device should operate according to the adaptive comfort model proposed by ANSI/ASHRAE 55. This model is applicable to naturally ventilated buildings controlled by occupants. According to this model, a 7-degree fluctuation of the indoor operative temperature grants 80% thermal acceptability [13]. The shading device should allow for direct sunlight when the operative temperature ( $T_o$ )<sup>2</sup> is below the temperature of the comfort zone (no shading or 0% shaded window). In the same way, the shading device should provide shade (50% and 100% shading) whenever  $T_o$  reaches the temperature of the comfort range or surpasses the upper threshold temperature. The system verifies indoor illuminance levels by adjusting the shading pattern post the evaluation of the thermal conditions. The thermal comfort parameters do not overlap.

### 3.3 Daylight Control

Before defining the luminous metric, it is necessary to check the potential illuminance distribution in the test cell. This analysis was performed using Relux<sup>3</sup>. As the shading system receives sensor signals from a point inside the test cell (during the physical monitoring process), the reference plane adopted in the daylight availability simulation was set at the height of 60 cm above a floor to prevent the direct bombardment of sunlight on the light sensor that could potentially affect subsequent measurements.

CIE clear-sky conditions were considered during the calculations. Hence, the shading system is simulated to manage direct sunlight. Figure 5 illustrates the distribution at noon at the reference plane during the summer and winter solstices (June 21 and December 21, respectively). The X and

---

<sup>2</sup>. Operative temperature: "the uniform temperature of an imaginary black enclosure, and the air within it, in which an occupant would exchange the same amount of heat by radiation plus convection as in the actual nonuniform environment" [13].

<sup>3</sup>. Relux is a free software for lighting analysis. The application library embeds national and international standards for real-time lighting and sensor simulation [14].

Y axes represent the test-cell internal dimensions, starting from 0.1 m, from the left corner of the façade with the window. The illuminance in the reference plane (at 0.60 m) is distributed according to a 0.20 m × 0.20 m grid, which is 0.10 m away from all sides. The window is located at the bottom, and the south orientation of the façade is simulated.

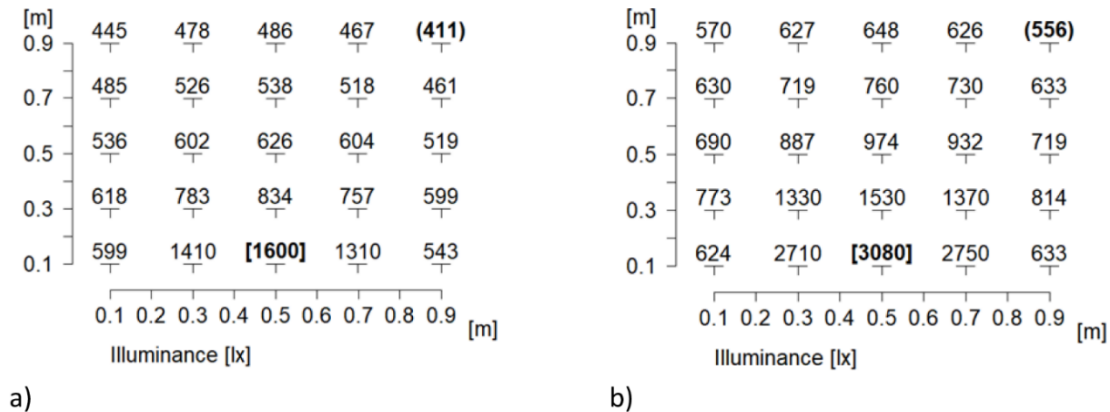


**Figure 5** Distribution of illumination during summer (a) and winter (b) solstices.

Analysis of the illuminance distribution reveals that in summer (Figure 4A), the availability ranges from a minimum of 411 lx (opposite side of the window) to a maximum of 1600 lx (the central point on the window sill). In winter (Figure 5B), the minimum level corresponds to 556 lx, and the maximum level is 3080 lx. During the summer months, under conditions of high solar angles, the need for shading is significantly diminished.

### 3.4 Illuminance Metric

The responsive shading system should be able to control the required indoor illuminance levels (we studied an office-like condition as a surrogate environment for the small internal space of the test cell). As the shading system should function under shading and direct sunlit conditions, the illuminance metric used for physical measurements should consider large variations between the minimum and maximum (allowed) illuminance levels.

The illuminance for the case of Useful Daylight Illuminance (UDI) proposed by Nabil and Mardaljevic [15] ranges from 100 to 2000 lx for daylit offices. Those thresholds were based on reports on the preferences of users working in environments equipped with non-automated shading devices.

Results obtained using Relux reveal that the indoor illumination in the test cell can range between 411 lx and 3080 lx between solstices at a reference hour (noon). Therefore, the UDI metric seems to fit well. However, direct sunlight at the desk level might cause user discomfort under real application conditions [11]. An alternative way to deal with this issue is to provide a flexible layout of the workstation to avoid the entry of direct sunlight on the work plane. This behavior is consistent with the concept of an adaptive zone, where users reduce the degree of glare to improve visual comfort. This is achieved by changing the position and view orientation during the day [16].

#### 4. Thermal Simulation using EnergyPlus

Simplified thermal simulations for responsive systems were performed using Energy Plus. In this case, the aforementioned guiding equations have not been taken into account, but instead, an ‘on/off’ operation was used. It was assumed that the absence and presence of shading characteristics were achieved at a fixed obstruction angle of the slats. Moreover, the adaptive comfort approach was not used. Instead, for the sake of simplification, a fixed setpoint temperature was adopted as a trigger to realize responsive shading.

##### 4.1 Simulation Procedure

A model was generated for a test building environment. A 9'6" high-cube shipping container with a floor area of approximately 5.4 m<sup>2</sup> was used to comply with the Brazilian thermal performance standards for office environments. Thermal transmittance of 0.87 W/m<sup>2</sup>K characterizes the walls and roofs. The suspended floor (the office-like space sits on top of a central axis that allows full rotation of the window according to different cardinal orientations) is characterized by a U-value of 1.00 W/m<sup>2</sup>K. The heat capacity is approximately 120 kJ/m<sup>2</sup>K. A double-glazing effect characterizes the window, and north-facing windows were used for thermal simulations. All surfaces are characterized by low solar absorptivity for white-painted buildings. Figure 6 illustrates the test environment used in this step.

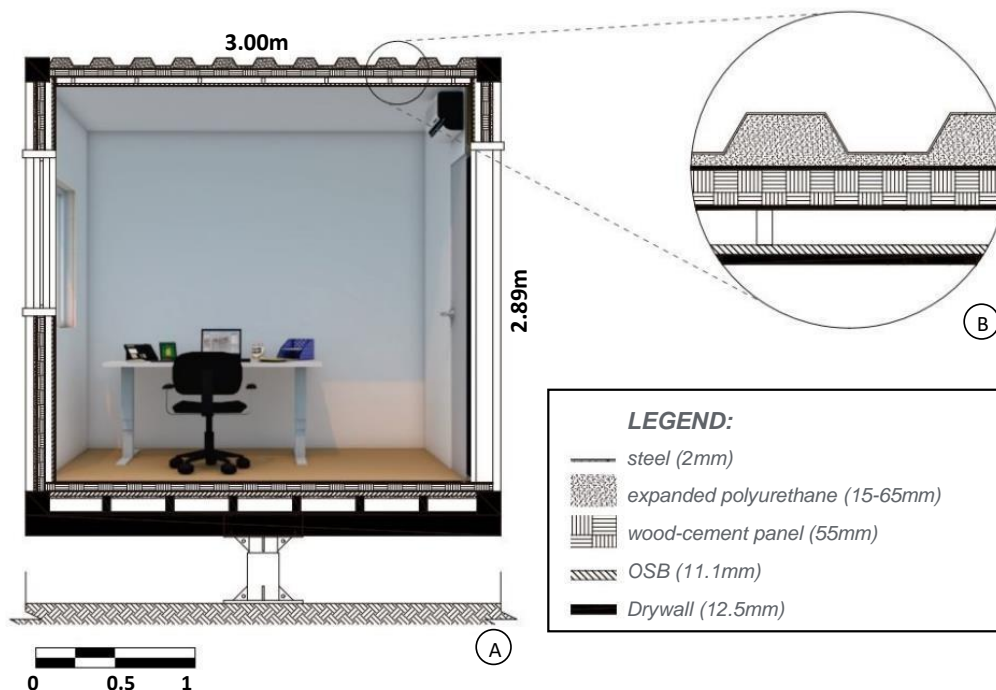


**Figure 6** Test environment - section (a); construction details (b).

Simulations were run for three different climatic regions of Brazil: the southern region, represented by the city of Curitiba (25.5 °S, 49.3 °W), the midwestern region, represented by the city of Brasília (15.8 °S, 47.9 °W), also the capital of the country, and the northeastern region, represented by Picos (7.1 °S, 41.2 °W), which is among the hottest cities in the country. In climatic terms, according to Köppen–Geiger’s climate classification, we have three distinct classes, namely

Cfb, Aw, and Bsh. The three places are located in different bioclimatic zones (ZB1, ZB4, and ZB7, respectively) [17, 18]. The three cities have significant climatic differences, ranging from a subtropical temperate climate (Curitiba), a tropical climate (Brasília), to the hot-dry climate of Picos.

The shading elements were dimensioned using the solar charts for the respective latitudes. The required projection angles, length, and spacing required between the slats were defined (Table 1).

**Table 1** Details of the dimensions of the shading elements, per location.

| Location | $\Theta$ (louver slat's tilt angle) (°) | Quantity of slats | louver slat's depth (BA) (m) | distance between slats (BC) (m) |
|----------|---|-------------------|------------------------------|---------------------------------|
| Curitiba | 25                                      | 3                 | 0.14                         | 0.30                            |
| Brasília | 40                                      | 3                 | 0.25                         | 0.30                            |
| Picos    | 60                                      | 4                 | 0.39                         | 0.23                            |

Four simulation scenarios were tested: 1) base case, with unobstructed window - without any shading elements; 2) simulation with fixed, static shading element throughout the year; 3) simulation with a shading element only in the summer period (retractable elements); 4) simulation with responsive shading taking into account the temperature parameter. In the case of the latter, the shading element was activated when the indoor temperature exceeded a setpoint temperature of 25 °C [19].

The model was generated and the dynamic thermal simulations were then performed using DesignBuilder and EnergyPlus (EP), respectively. All simulation runs were performed on an annual basis, and the climate data were obtained from the EP database. The simulation parameters were presented: no occupation; no internal gains; use of shading elements (when applicable, according to the predefined simulation scenarios); free-running mode with 1 ACH in winter, 7 ACH in summer, and 4 ACH in shoulder seasons, with window orientation to true north.

Simulations were performed for each scenario for each city, allowing an overall analysis of thermal behavior based on the seasons of the year. Indoor thermal comfort was assessed according to EN 15251 [20].

## 5. Results and Discussion

Shading simulations presented here were run at 09:00 am, 12:00 pm, and 03:00 pm on December 21 (winter solstice). As the shading equation solely considers the solar altitude for defining whether shading needs to be applied, the conditions of 50% and 0% shading are more accurate at noon, when the sun's position is at an azimuth of 180 ° (to the south). Figure 7, Figure 8, and Figure 9 present the shading patterns observed indoors (December 21 at 9 am, noon, and 3 pm). The simulations for the remaining months are presented in Figure S1 and Figure S2 (Additional material). Simulations were carried out for the case of noon on the 21<sup>st</sup> day of December.



**Figure 7** Shading pattern, December 21<sup>st</sup> at 09:00 am (0%, 50%, and 100% shading).



**Figure 8** Shading pattern, December 21, at 12:00 pm (0%, 50% and 100% shading).



**Figure 9** Shading pattern, December 21 at 03:00 pm (0%, 50%, and 100% shading).

According to definition, the shading device creates three distinct conditions: 0% shading, allowing the entry of an amount of direct sunlight that roughly corresponds to the window area, excluding the thickness of the louver slats; 50% shading, which reduces the visible light to half of the window area, in a striped shading pattern; and 100% shading when direct sunlight does not enter, and the external view is not blocked. As shown in Figure 7, Figure 8, and Figure 9, the outdoor view can be obtained when 50% and 100% of the window is shaded. Finally, solar heat gains and illuminance levels tend to reduce under these conditions.

An advantage of using the proposed shading patterns associated with a responsive shading device is the ability to effectively adjust the entry of sunlight and indoor illuminance throughout the seasons. As shown in Figure S1 and Figure S2 (Additional Material), the responsive device will be able to adjust direct sunlight from August to April (through nine months) when sunlight directly enters the rooms. This happens approximately 75% of the year. However, the effectiveness of the shading control mechanism becomes more evident when the solar angles are lower, that is, from October to February (41% of the months). For the remaining months, especially during summer (when the solar angles are higher), the responsive shading device will work as a diffuse solar radiation controller, primarily focused on indoor illuminance.

Thermal performance and comfort analysis results are shown in Figure 10, Figure 11, and Figure 12. The results represent the percentage of annual daytime hours (from 6 am to 6 pm, to account for the differences in thermal comfort attributable to differing shading profiles) corresponding to thermal comfort and thermal discomfort. The results were obtained for the cold or heat conditions for the three locations. The calculations were made based on the guidelines of the European Standard EN 15251 [20]. The lower limit for indoor thermal comfort range is 20 °C, while the upper limit is 25 °C.

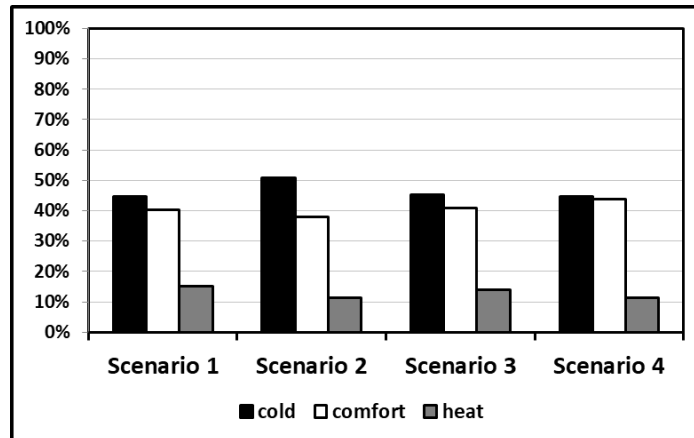


**Figure 10** Percentage of comfort, cold, and hot discomfort during the day (annual calculations; EN 15251 limits – Curitiba).

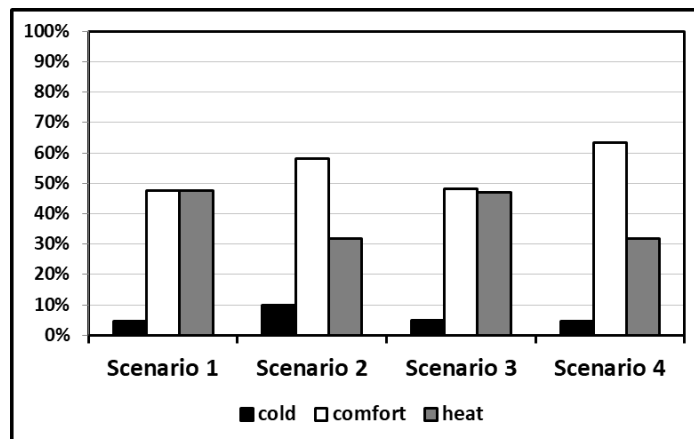


**Figure 11** Percentage of hours of comfort, cold, and hot daytime discomfort (annual calculations; EN 15251 limits - Brasília).

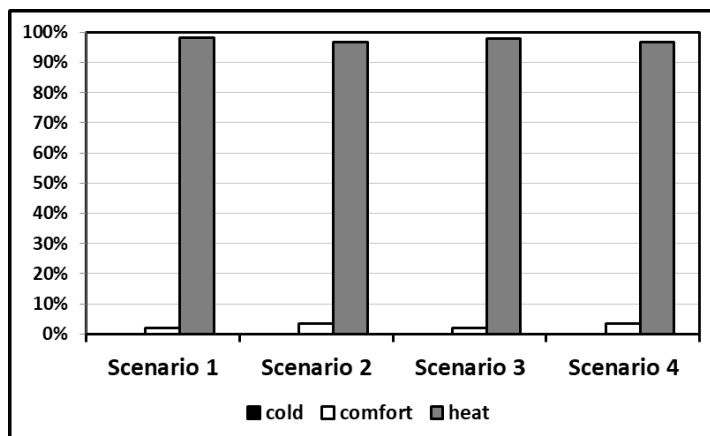


**Figure 12** Percentage of comfort, cold, and hot discomfort during the day (annual calculations; EN 15251 limits – Picos).

The scenario that yielded the best performance in all the cities, in terms of thermal comfort and, consequently, in terms of curbing energy demand for cooling, was scenario IV (responsive shading elements). Table 2 presents the hours of comfort/discomfort for each case.

**Table 2** Comfort, cold, and hot discomfort daytime hours (annual calculations) and the percent changes relative to the base case.

| Location | Scenario   | cold | comfort | heat | % Reduction (cold) to base case scenario | % Increase (comfort) to base case scenario | % Reduction (overheating) to base case scenario |
|----------|------------|------|---------|------|--|--|---|
| Curitiba | Scenario 1 | 2126 | 1908    | 711  | -  | -  | -   |
|          | Scenario 2 | 2405 | 1804    | 536  | -13%                                     | -5%  | -25%  |
|          | Scenario 3 | 2142 | 1937    | 666  | -1%                                      | 2%   | -6%   |
|          | Scenario 4 | 2126 | 2083    | 536  | 0%                                       | 9%   | -25%  |
| Brasília | Scenario 1 | 220  | 2262    | 2263 | -  | -  | -   |
|          | Scenario 2 | 473  | 2761    | 1511 | -115%                                    | 22%  | -33%  |
|          | Scenario 3 | 232  | 2287    | 2226 | -5%                                      | 1%   | -2%   |
|          | Scenario 4 | 220  | 3014    | 1511 | 0%                                       | 33%  | -33%  |
| Picos    | Scenario 1 | 0    | 86      | 4659 | -  | -  | -   |
|          | Scenario 2 | 0    | 158     | 4587 | -  | 84%  | -2%   |
|          | Scenario 3 | 0    | 93      | 4652 | -  | 8%   | 0%  |
|          | Scenario 4 | 0    | 158     | 4587 | -  | 84%  | -2%   |

Scenario I (no shading, baseline scenario) and scenario IV (with responsive shading elements) are directly compared, and the largest percent reduction in overheating conditions is verified for Brasília (with a drop of one-third of the overheating hours in scenario IV). Compared to scenario II (static shading), no changes in this parameter were observed. In Brasília, the responsive shading element is advantageous as it does not lead to increased heating needs. The static shading scenario blocks the desired heat gains through the window during the cold periods of the year. Scenario III, with seasonal shading, performs poorer than the case where responsive shading is

adopted. However, it performs much better than Scenario II but is ineffective in controlling overheating throughout the year. Similar results are obtained for Curitiba. In this case, the ability to resist cold stress decreases (the results obtained when scenarios IV and II are directly compared).

In Picos, hot weather is well distributed throughout the year, and there are no defined seasons. Hence, responsive shading is not an effective alternative compared to static shading (scenario II) (as there is a year-round need for shading).

In summary, in terms of comfort, responsive shading systems are expected to be more effective in places that have defined seasons. For example, in tropical climates with a significant year-round need for shading, such systems will not have an additional advantage over static shading devices.

## **6. Conclusions**

Provided that the responsive shading system is programmed to shade the desired window or indoor area according to the established solar positions determined by studying solar geometry and predefined indoor conditions (temperature, light), it has the potential to improve IEQ while decreasing energy demand for cooling and electric lighting. In climates characterized by sudden variations of atmospheric conditions, a dynamic, responsive shading system will less likely lead to unnecessary shading and thus reduce cold discomfort. In subtropical regions, the potential of such a system for increasing IEQ is expected to be high.

The guiding rules of the responsive shading system proved to be satisfactory when 3D simulation analysis was performed. The solar azimuth position should be studied every hour to obtain an accurate and dynamic shading pattern adjustment method. In addition, the system strategy for different latitudes and façade orientations should also be studied.

Appropriate adjustments to the programming rules should include the rotation of the base-slats to redirect the airflow at night in the case of selective, nocturnal ventilation. In the same way, during rainy days, the shading system should adjust the slats to prevent the entry of rainwater when windows are kept open to allow cross ventilation and a view of the outside.

Thermal simulation results revealed that the responsive shading system performs well in locations with well-defined seasons. From the thermal comfort point of view, when compared to seasonal shading devices (e.g., when retractable awnings or deciduous trees are used), responsive shading systems can account for sudden changes in atmospheric conditions due to weather instabilities and cold fronts. These are common at higher latitudes in Brazil. Furthermore, dynamic control of window shading prevents unwanted heat gains and unnecessary window shading at times.

The physical implementation of the shading device and the monitoring of indoor conditions (temperature and illuminance levels) were carried out to verify the efficiency of the shading device. Once the system is implemented, the next stage will be to evaluate users' satisfaction of users and the level of possible sources of disturbance created by the system itself. Anticipated issues that could arise from the operation of the dynamic shading system are the noise generated by the motor attached to the brise slats and the contrasting and sudden light situations during the operation of the device (under conditions of low or highly intense light). These situations should be studied to improve the devices and the operation schedules (setpoints, intervals between readings, etc.).

## **Acknowledgments**

We want to thank Prof. Leandro Fernandes, from the Federal University of Paraná, Brazil, for the design concept support and the shading pattern strategy suggestion.

## **Author Contributions**

Eduardo Krüger and Pablo La Roche supervised the research development, contributed to the analysis, and revised the manuscript. Marlon Mülhbauer developed the shading equations and the respective article topic. Gabriel de Bem conceived, developed the research simulations, and was responsible for the preparation of the manuscript. André Matias was responsible for the thermal simulations in EP, under the supervision of Ricardo Almeida. All authors contributed to the final revision of the paper.

## **Funding**

This study was funded in part by the Coordenação de Aperfeiçoamento de Pessoal de Nível Superior – Brasil (CAPES) – Finance Code 001 and Lyle Center for Regenerative Studies.

## **Competing Interests**

The authors have declared that no competing interests exist.

## **Additional Materials**

The following additional materials are uploaded at the page of this paper.

1. Figure S1: Shading Simulation from January 21<sup>st</sup> to June 21<sup>st</sup>.
2. Figure S2: Shading Simulation from July 21<sup>st</sup> to December 21<sup>st</sup>.

## **References**

1. Achten H. Interaction narratives for responsive architecture. *Buildings*. 2019; 9: 66.
2. Thun G, Velikov K. North house: Prototyping climate responsive envelope and control systems. *Res J*. 2013; 5: 39-54.
3. Meagher M. Designing for change: The poetic potential of responsive architecture. *Front Archit Res*. 2015; 4: 159-165.
4. Heidari Matin N, Eydgahi A. A data-driven optimized daylight pattern for responsive facades design. *Intell Build Int*. 2022; 14: 363-374.
5. La Roche P, Murray M. Effects of combining smart shading and ventilation on thermal comfort. *Proceedings of the 2005 solar world congress: Bringing water to the world, including proceedings of 34th ASES Annual Conference, 30th National Passive Solar Conference; 2005 August 8th-12th; Orlando, FL, USA*. Washington: International Solar Energy Society.
6. Kuczyński T, Staszczuk A, Gortych M, Stryjski R. Effect of thermal mass, night ventilation and window shading on summer thermal comfort of buildings in a temperate climate. *Build Environ*. 2021; 204: 108126.
7. Phillips D. *Daylighting: Natural light in architecture*. Oxford: Architectural Press; 2004. p. xxi.

8. Ruck N, Aschehoug Ø, Aydinli S, Christoffersen J, Courret G, Edmonds I, et al. Daylight in Buildings: A sourcebook on daylighting systems and components. Berkeley; CA: Lawrence Berkeley National Laboratory; 2000. p. 29.
9. IEA. Tracking buildings 2021 [Internet]. Paris: International Energy Agency; 2021 [cited date 2022 May 3rd]. Available from: <https://www.iea.org/reports/tracking-buildings-2021>.
10. Ricci A, Ponzio C, Fabbri K, Gaspari J, Naboni E. Development of a self-sufficient dynamic façade within the context of climate change. Archit Sci Rev. 2020; 64: 87-97.
11. Reinhart C. Daylighting Handbook I: Fundamentals; designing with the sun. Cambridge: Building Technology Press; 2020. p. 23.
12. Trimble. Why SketchUp [Internet]? Sunnyvale: Trimble Inc.; 2022 [cited date 2022 May 10th]. Available from: <https://www.sketchup.com/why-sketchup>.
13. American Society of Heating, Refrigerating, and Air-Conditioning Engineers. ASHRAE Standard 55-2020—Thermal environmental conditions for human occupancy [Internet]. Atlanta: American Society of Heating, Refrigerating, and Air-Conditioning Engineers, Inc.; 2020. Available from: <http://arco-hvac.ir/wp-content/uploads/2015/11/ASHRAE-55-2010.pdf>.
14. Relux. Relux desktop—The new free approach to planning [Internet]. Münchenstein: Relux Informatik AG; [cited date 2022 May 12th]. Available from: <https://reluxnet.relux.com/en/>.
15. Nabil A, Mardaljevic J. Useful daylight illuminance: A new paradigm for assessing daylight in buildings. Light Res Technol. 2005; 37: 41-57.
16. Jakubiec JA, Reinhart CF. The adaptive zone—A concept for assessing discomfort glare throughout daylit spaces. Light Res Technol. 2012; 44: 149-170.
17. Peel MC, Finlayson BL, McMahon TA. Updated world map of the Köppen-Geiger climate classification. Hydrol Earth Syst Sci. 2007; 11: 1633-1644.
18. Associação Brasileira de Normas Técnicas. NBR 15220 Parte 3: Zoneamento bioclimático brasileiro Origem: Projeto 02:135.07-001/3:2003 ABNT/CB-02—Comitê Brasileiro de Construção Civil CE-02:135.07—Comissão de Estudo de Desempenho Térmico de Edificações. Associação Brasileira de Normas Técnicas; 2003.
19. Decreto-Lei n.º 101-D/2020, Diário da República n.º 237/2020, 1º Suplemento, Série I de 2020-12-07. Diário da República; 2020. pp. 21-45.
20. Comitê Europeu De Normalização. Indoor environmental input parameters for design and assessment of energy performance of buildings addressing indoor air quality, thermal environment, lighting and acoustics. Comitê Europeu De Normalização; 2006; prENrev 15251:2006 (E).



Enjoy *AEER* by:

1. [Submitting a manuscript](#)
2. [Joining in volunteer reviewer bank](#)
3. [Joining Editorial Board](#)
4. [Guest editing a special issue](#)

For more details, please visit:

<http://www.lidsen.com/journals/aeer>